Retrospective Clinical Research Report

Journal of INTERNATIONAL MEDICAL RESEARCH

Journal of International Medical Research
48(5) 1–12

DOI: 10.1177/0300060520924250
journals.sagepub.com/home/imr
SAGE

Traditional three-dimensional printing technology versus three-dimensional printing mirror model technology in the treatment of isolated acetabular fractures: a retrospective analysis

Cong Yu[1,*], Weiguang Yu[2,*], Shuai Mao[3], Peiru Zhang[1], Xinchao Zhang[4], Xianshang Zeng[2] and Guowei Han[2]

Abstract

Objective: This study was performed to compare the clinical outcomes of traditional three-dimensional (3D) printing technology and 3D printing mirror model technology in the treatment of isolated acetabular fractures.

Methods: Prospectively maintained databases were reviewed to retrospectively compare patients with an isolated acetabular fracture who were treated with traditional 3D printing technology (Group T) or 3D printing mirror model technology (Group M) from 2011 to 2017. In total, 146 advanced-age patients (146 hips) with an isolated acetabular fracture (Group T, n = 72; Group M, n = 74) were assessed for a mean follow-up period of 29 months (range, 24–34 months). The primary endpoint was the postoperative Harris hip score (HHS). The secondary endpoints were the operation time, intraoperative blood loss, fluoroscopy

[1]Department of Anesthesiology, Wuhan Fourth Hospital; Puai Hospital, Tongji Medical College, Huazhong University of Science and Technology, Wuhan, China
[2]Department of Orthopaedics, The First Affiliated Hospital, Sun Yat-sen University, Guangzhou, China
[3]Department of Hepatobiliary Surgery, The First Affiliated Hospital, Sun Yat-sen University, Guangzhou, China
[4]Department of Orthopaedics, Jinshan Hospital, Fudan University, Shanghai, China

*These authors contributed equally to this work.

Corresponding author:
Peiru Zhang, Department of Anesthesiology, Wuhan Fourth Hospital; Puai Hospital, Tongji Medical College, Huazhong University of Science and Technology, Hanzheng Street No. 473, Qiaokou District, Wuhan, 430033, China.
Email: peiru0124@163.com
Xianshang Zeng, Department of Orthopaedics, The First Affiliated Hospital, Sun Yat-sen University, No. 58, Zhongshan 2nd Road, Yuexiu District, Guangzhou, 510080, China.
Email: xianshangzh@126.com

screening time, fracture reduction quality, and incidence of postoperative complications at the final follow-up.
Results: The HHS, operation time, intraoperative blood loss, fluoroscopy screening time, and incidence of postoperative complications were significantly different between the groups, with Group M showing superior clinical outcomes.
Conclusion: In patients with an isolated acetabular fracture, 3D printing mirror model technology might lead to more accurate and efficient treatment than traditional 3D printing technology.

Keywords
Three-dimensional, mirror model technology, acetabular fracture, Harris hip score, printing technology, advanced age

Date received: 11 December 2019; accepted: 14 April 2020

Background

Acetabular fracture is usually considered to involve high-energy injuries of the hip joint. These fractures affect patients worldwide and are associated with high morbidity.[1–3] The incidence of acetabular fractures and associated mortality in China has been increasing since 2007.[4–6] Current approaches to the treatment of acetabular fractures have achieved important advances but remain in need of significant improvement.[7–9] Furthermore, for patients with acetabular fractures with obvious displacement, the preferred surgical approach is anatomic reduction, strong internal fixation, and early functional exercise to maximize the chance of a good functional outcome.[10,11] However, because of the deep anatomical position of acetabular fractures, limited ability to directly manufacture fixation devices, and anatomic complexity of the fracture regardless of the soft tissue structures, the current approaches are associated with many difficulties. These difficulties include severe surgical trauma, a complicated operation, and temporary pre-bending of the plate during surgery, resulting in a prolonged operation time, aggravated soft tissue trauma, and increased intraoperative blood loss. All of these factors have been regarded as important prognostic indicators of the surgical outcome.[3,12–14]

The 3D-printed model only mimics the surface structure of the real bone and has a solid infill. In recent years, however, 3D printing has gained the ability to fabricate complex geometries, primarily based on selective laser sintering of ceramic or thermoplastic microparticles. This has resulted in a remarkable growth potential for orthopedic-assisted devices and provides a basis for personalized fracture management.[15–17] Human bones are generally symmetrical in shape; that is, they exhibit a mirror relationship. To obtain 3D morphological information before acetabular fracture repair, we used computed tomography (CT) medical imaging data of the contralateral acetabulum to form the 3D-printed structure (3D printing mirror model technology), which is the normal model of the affected acetabulum. We used the new 3D printing mirror model as a benchmark for surgical predrilling and determined the position and pre-bending properties of the pelvic reconstruction plate and the length of the screws.

This study was performed to compare the clinical outcomes of traditional 3D printing technology and 3D printing

mirror model technology for the treatment of isolated acetabular fractures.

Methods

Study design and patient eligibility

Institutional review board approval was obtained from Wuhan Fourth Hospital; Puai Hospital, Tongji Medical College, Huazhong University of Science and Technology, Wuhan, China and included an exemption from the requirement for informed consent. We conducted a retrospective review of prospectively gathered data from our medical center from June 2011 to December 2017, in which consecutive patients who underwent traditional 3D printing technology or 3D printing mirror model technology following an isolated acetabular fracture were identified by the International Classification of Diseases (10th revision). Follow-up was initiated at the onset of the first day after primary acetabular fracture surgery. The inclusion criteria were a unilateral isolated acetabular fracture, fresh acetabular fracture with a $\leq$2-week duration from injury to operation, no hip joint dysfunction or deformity before the fracture, and the ability of the patient to comprehend instructions and follow a rehabilitation program. The exclusion criteria were severe nerve and vascular injury of the ipsilateral lower limbs, bilateral acetabular fractures, non-isolated acetabular fractures, pathological fractures, severe osteoporosis, open fractures, severe circulatory diseases, incomplete clinical or radiographic data, severe organ failure, uncontrolled metabolic dysfunction, loss to follow-up or refusal to participate, lack of healing after surgery, a high risk of bleeding, Injury Severity Score of $\geq$9, severe medical disease, advanced cancer, co-occurring mental illness, cognitive dysfunction, New York Heart Association classification of 3, and American Society of Anesthesiologists score of IV or V.

Surgical technique

Preoperative management. All patients underwent supracondylar femoral traction or skin traction after admission according to their fracture type and were examined by color Doppler ultrasound, pelvic radiographs, plain CT, and 3D CT reconstruction. The amount of blood prepared before surgery was 400 to 600 mL. Before surgery, nonsteroidal anti-inflammatory drugs were provided for pain relief. All patients received 2.0 g of cefazolin sodium (1.0 g; Sigma-Aldrich, St. Louis, MO, USA) to prevent infection 30 to 60 minutes before the start of surgery.

We performed data processing using Mimics 15.0 software (Materialise NV, Leuven, Belgium) and removed unnecessary structures such as the femoral head, sacrum, and coccyx by threshold segmentation to obtain an uncovered acetabular panorama. For Group T, in which traditional 3D printing technology was used, we directly generated 3D images of the affected acetabulum. For Group M, in which mirror model technology was used, we generated a 3D image of the affected acetabulum as well as a new 3D image of the contralateral acetabulum (Figure 1(a)–(c)). We exported two sets of 3D images into STL format files, sliced and supported the 3D images by Cura software (Ultimaker, Geldermalsen, Netherlands), converted them into CODE format files that could be recognized by 3D printers, imported them into 3D printers, and printed the fracture models using Objet MED610 polymer (Stratasys Inc., Rehovot, Israel) at a 1:1 ratio. The printing process has been previously described.[5]

Intraoperative management. For Group T, we removed the supports between the 3D model bones and dissociated each fragment to

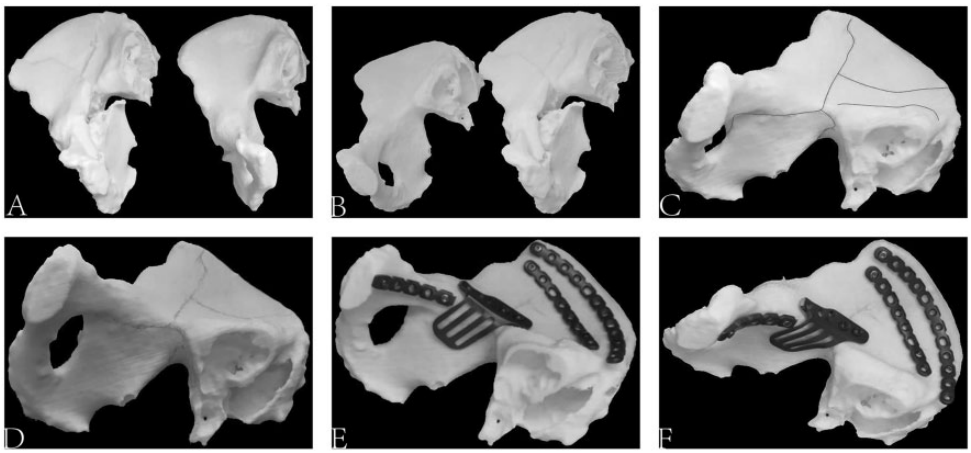

Figure 1. Radiographic images. (a) Preoperative pelvic radiograph (anteroposterior view) taken at the time of initial presentation revealing a right acetabular fracture (both columns). (b and c) Intraoperative fluoroscopic images of the right acetabular fracture based on three-dimensional printing mirror model technology. (d) Postoperative pelvic radiograph (anteroposterior view) and (e) anterior and (f) lateral images of the femur showing the placement of the implants.

intuitively and accurately understand the fracture situation. We reset the fracture model and temporarily fixed it with a Kirschner wire if necessary. After obtaining satisfactory results, we selected the appropriate reconstruction plate (Synthes Inc., West Chester, PA, USA), pre-bent it to fit the bone surface, and adjusted it to the appropriate position; we then determined the specification and model of the reconstruction plate, the direction and length of the fixation screw, and the relationship of the acetabular joint. For Group M, we selected the appropriate reconstruction plate, pre-bent it to fit the bone surface, and adjusted it to the appropriate position; we then determined the specification and model of the pelvic reconstruction plate, the direction and length of the fixing screw, and the relationship of the acetabular joints (Figure 1(d)–(f)).

According to the type and nature of the acetabular fracture, the patient was placed in either the supine or lateral position under general anesthesia and treated with either the Kocher–Langenbeck or modified Stoppa approach. According to the preoperative plan, we completed the reduction as soon as possible, placed the pre-bent pelvic reconstruction plate in the position that had been established during the rehearsal, ensured that the plate and bone surface fit well, temporarily fixed the position, and inserted the appropriate screw into the predesigned screw trajectory on the 3D model to provide absolute stability of fracture reduction. C-arm images were viewed in multiple planes to certify anatomic reduction (Figure 2(a)–(f)). Immediate revision was carried out if necessary. The same group of orthopedic surgeons operated on the patients in both groups.

Postoperative management. An antibiotic (cefazolin sodium 2.0 g) was routinely given for 2 days postoperatively. Sequential compression stockings were used to prevent venous thromboembolism, starting the first day postoperatively and continuing for at least 21 days. A once-daily injection of enoxaparin (Clexane, 4000 aXa IU; Sanofi, Hangzhou, China) was administered as early as 6 hours postoperatively for 7

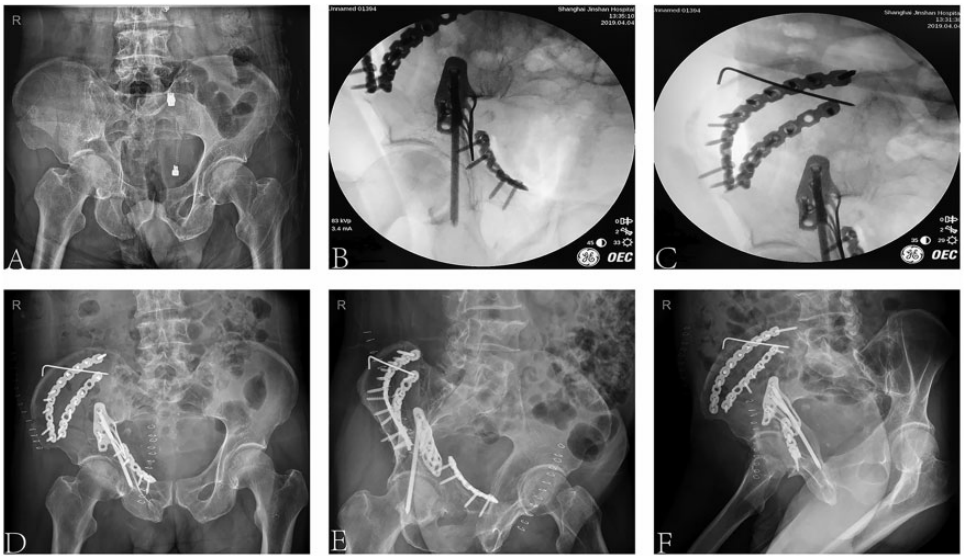

Figure 2. Three-dimensional printed model. (a and b) Three-dimensional printed model of the bilateral acetabula providing an understanding of the normal three-dimensional anatomy of the pelvic brim and acetabular columns. (c and d) Shape and orientation of the fracture line being indicated by scribing on the mirror model. (e and f) Three-dimensional printed model with plate applied.

subsequent days. The incision drain was removed when <30 mL of drainage fluid was noted over 24 hours. Depending on the patient's tolerance, functional muscle contraction training was initiated as soon as possible. On the first day postoperatively, continuous passive motion (CPM device; Smith & Nephew, London, UK) was carried out. Active exercises after drain removal were initiated. Touch-down weight-bearing of the affected limb was encouraged with a walker between 2 and 30 days after surgery and with crutches between 30 and 90 days. Full weight-bearing was allowed after 90 days according to the patient's clinical and radiological evidence. The overall rehabilitation protocol was identical for all patients.

Statistical analysis

The patients were reviewed clinically and radiographically at 1, 3, 6, 9, and 12 months postoperatively and yearly thereafter. The assessment of the acetabular fracture type was based on the Letournel–Judet classification.[2,6] The operation time was defined as the time from reduction of the bone fragment to optimal placement of the internal fixation device. The amount of intraoperative blood loss was calculated as previously described.[18–21] The intraoperative fluoroscopy screening time was defined as the duration of intraoperative observation of fracture reduction or internal fixation. Hip function was evaluated using the Harris hip score (HHS). The quality of the reduction was assessed by Matta's criteria.[14] Heterotopic ossification was assessed by the Brooker classification system.[21] Loosening, bone union, malunion, and nonunion were defined as previously described.[20–22] Revision was defined as exchange of a part or the whole implant or as removal of the implant.[22] Implant failure occurred when surgical intervention was necessary for acetabular fractures with a change of the implant.[20] The results are expressed as mean with standard deviation

Table 1. Patient demographics and outcomes.

Variable	Group T (n = 72)	Group M (n = 74)	*p*-value
Sex, male/female	32/40	30/44	0.633[a]
Age, years	71.34 ± 8.15	71.65 ± 7.76	0.241[b]
BMI, kg/m^2	26.59 ± 9.28	26.84 ± 8.75	0.425[b]
BMD	−2.46 ± 0.73	−2.83 ± 0.57	0.326[b]
Side, left/right	44/28	41/33	0.485[a]
Comorbidities			0.590[c]
Hypertension	21	20	
Diabetes mellitus	20	18	
Hypertension and diabetes mellitus	6	7	
Pulmonary	8	10	
Cerebrovascular accident	6	7	
Cardiopathy	6	5	
Anemia	5	7	
Mechanism of injury			0.576[c]
Traffic-related injury	40	43	
Injury by falling	21	24	
Tamping injury	11	7	
ASA score			0.460[c]
I	11	14	
II	32	34	
III	29	26	
Fracture types			0.605[c]
Associated both-column	21	18	
Transverse + posterior wall	16	19	
T-shaped	13	12	
Transverse	8	9	
Anterior column	4	3	
+ Posterior hemitransverse	3	5	
Posterior column + posterior wall	7	8	
Operation position			0.630[c]
Supine	34	32	
Lateral	38	42	
Approach			0.770[c]
Kocher–Langenbeck	47	50	
Modified Stoppa	25	24	
Time to surgery, days	9.00 ± 6.00	9.00 ± 7.00	0.317[b]
Preoperative HHS	53.23 ± 11.59	53.44 ± 10.36	0.617[b]
Follow-up period, months	29.16 ± 4.21	29.21 ± 4.77	0.425[b]

Data are presented as mean ± standard deviation or number of patients

[a]Analyzed using the chi-square test; [b]Analyzed using the independent-samples t-test; [c]Analyzed using the Mann–Whitney test.

Group T, traditional three-dimensional printing technology; Group M, three-dimensional printing mirror model technology.

HHS, Harris hip score; ASA, American Society of Anesthesiologists; BMI, body mass index; BMD, bone mineral density.

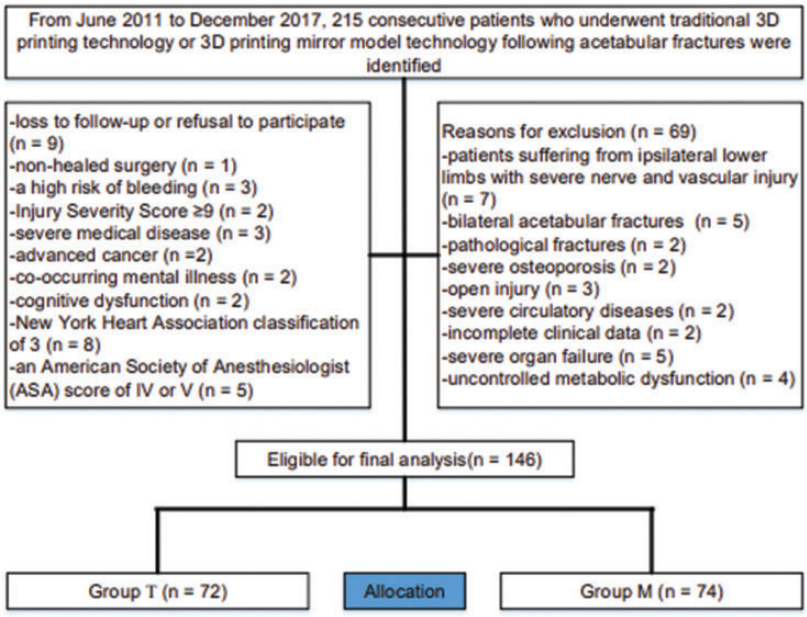

Figure 3. Study flow diagram, including reasons for exclusion. 3D, three-dimensional; Group T, traditional three-dimensional printing technology; Group M, three-dimensional printing mirror model technology.

or median with interquartile range. The chi-square test or Fisher's exact test was used to analyze categorical variables. Between-group differences were assessed using Student's t-test or the Wilcoxon rank sum scores for continuous variables. A two-sided p value of <0.05 was considered statistically significant. Data analysis was performed using SPSS version 24.0 (IBM Corp., Armonk, NY, USA).

Results

In total, 215 patients who underwent treatment using traditional 3D printing technology or 3D printing mirror model technology were assessed for study eligibility. Of these, 146 patients from whom all relevant information was available met the inclusion criteria. Group T comprised 72 patients with a mean age of 71.34 ± 8.15 years, and Group M comprised 74 patients with a mean age of 71.65 ± 7.76 years. The mean follow-up duration was 29 months (range, 24–34 months). No statistically significant between-group differences were observed in the baseline data, which are summarized in Table 1. The study flow chart is shown in Figure 3.

Primary endpoint

Changes in the HHS from the preoperative period to the final follow-up in Groups T and M are shown in Table 2. At each follow-up point, the HHS in Group M was significantly higher than that in Group T ($p < 0.05$ for all). From 1 to 3 months postoperatively, the improvement in the HHS in Group M was significantly greater than that in Group T ($p < 0.05$). In Group T, the HHS was significantly lower at 12 months postoperatively than it had been at 9 months ($p < 0.05$); however, this difference was not observed in Group M. At the final follow-up, the improvement in

Table 2. Long-term follow-up primary endpoint.

HHS, months postoperatively	Group T (n = 72)	Group M (n = 74)	*p*-value
1	79.14 ± 6.42	81.33 ± 8.26	0.035*
3	81.58 ± 7.23	84.63 ± 8.55	0.027*
6	83.41 ± 8.36	85.17 ± 8.42	0.035*
9	84.21 ± 9.12	86.74 ± 7.40	0.026*
12	81.56 ± 7.79	86.69 ± 9.52	0.014*
15	81.74 ± 12.41	87.72 ± 11.15	0.011*
18	82.37 ± 11.24	87.56 ± 11.32	0.015*
21	81.69 ± 12.18	87.45 ± 12.59	0.013*
24	82.41 ± 13.27	86.58 ± 11.14	0.019*
Final follow-up	80.23 ± 13.14	86.42 ± 12.47	0.009*

Data are presented as mean ± standard deviation.
*Statistically significant values.
Group T, traditional three-dimensional printing technology; Group M, three-dimensional printing mirror model technology.
HHS, Harris hip score.

the HHS from baseline was significantly greater in Group M than T ($p = 0.000$).

Secondary endpoints

Significant between-group differences were found in the secondary endpoints of the operation time, intraoperative blood loss, fluoroscopy screening time, fracture reduction quality, and incidence of postoperative complications at the final follow-up, as shown in Table 3. The operation time by independent review (81.53 ± 9.86 vs. 91.46 ± 11.29 minutes; 95% confidence interval [CI], 0.32–0.35; $p = 0.001$), intraoperative blood loss (435.6 ± 65.36 vs. 542.4 ± 72.13 mL; 95% CI, 0.42–0.67; $p = 0.001$), fluoroscopy screening time (4.12 ± 0.54 vs. 5.63 ± 1.91; 95% CI, 0.14–0.37; $p = 0.016$), and number of anatomical reductions (50 vs. 33; 95% CI, 0.56–0.78; $p = 0.008$) were significantly better in Group M than T. Group M tended to be superior to Group T in terms of postoperative complications. Significant differences were detected with regard to implant loosening ($p = 0.005$), implant failure/revision ($p = 0.012$), and heterotopic ossification (III and IV) ($p = 0.001$). A consistent trend for the secondary endpoint benefit in Group M was more significant than that in Group T. The interaction between the secondary endpoints was not tested in our analysis.

Discussion

The results of this study involving patients with acetabular fractures treated with traditional 3D printing technology or 3D printing mirror model technology suggest that, similar to what was found in the primary analysis, 3D printing mirror model technology with highly detailed models of complex fractures and recreation of the preinjury anatomical morphology has significant advantages over traditional 3D printing technology. Despite being recognized as the standard of care in most patients with acetabular fractures in our medical institution, 3D printing mirror model technology may be insufficient in this setting.

Our findings are consistent with previous reports[1,5,7] and suggested that mirror model technology tends to improve the clinical outcomes for patients with acetabular

Table 3. Long-term follow-up secondary endpoints.

Variable	Group T (n = 72)	Group M (n = 74)	*p*-value
Operation time, minutes	91.46 ± 11.29	81.53 ± 9.86	0.001*
Intraoperative blood loss, mL	542.4 ± 72.13	435.6 ± 65.36	0.001*
Fluoroscopy screening time, minutes	5.63 ± 1.91	4.12 ± 0.54	0.016*
Fracture reduction quality			0.030*
Anatomical	33	50	
Imperfect	32	20	
Poor	7	4	
Postoperative complications			
Implant loosening	21	8	0.005*
Implant failure/revision	12	3	0.012*
Refracture	5	4	0.699
Femoral fracture	3	1	0.297
Lower limb shortening (>1.5 cm)	5	1	0.089
Heterotopic ossification (III and IV)	23	7	0.001*
Infection	8	6	0.538
Symptoms of nerve stimulation	1	1	0.984
Traumatic osteoarthritis	4	2	0.385

Data are presented as mean ± standard deviation or number of patients.
*Statistically significant values.
All p values were obtained by the chi-square test.
Group T, traditional three-dimensional printing technology; Group M, three-dimensional printing mirror model technology.

fractures. A retrospective study by Li et al.[4] involving 16 patients with traumatic posterior dislocation of the hip combined with acetabular fractures showed that 3D printing models had superior effectiveness and achieved an extremely tangible preoperative assessment of fractures compared with traditional surgery. Additionally, a prospective multicenter study[1] demonstrated that 3D models can enhance our understanding of the spatial relationship between anatomical landmarks and fracture lines. Why these analogous regimens translated into similar gains in clinical outcomes is comprehensible. A potential explanation for the better-than-expected clinical performance appears to be the choice of 3D model. At present, 3D printing technology is still in the development stage, with some disadvantages in terms of the poor accuracy of the printed model and the rough edges of the printed fragments.[23] The resolution and morphology of a print rely on various machine settings.[19,24] Direct observation of the spatial relationship between real fragments is limited.[12,24]

The human skeleton is generally bilaterally symmetric; this is known as a mirror relationship. This mirror relationship is the theoretical basis for using the contralateral acetabular mirror model as a template for the affected side. The mirror imaging model of the contralateral acetabulum replaces the post-reduction state of the affected acetabulum, which can greatly simplify the process of fracture assembly and reduction, improve the accuracy of reduction, and provide an excellent template for pre-bending of the pelvic reconstruction plate and determination of the screw length.[4] Because the shape of the pre-bent plate fits well with the fracture fragment after the reduction, the pre-bent plate can be used as the benchmark when

intraoperative reduction is difficult, and reduction is achieved by fitting the fracture end to the pre-bent reconstruction plate. The plate can be fixed with one side of the fracture end using a screw at the predetermined position; the plate and the other side of the fracture end can then be adjusted, reset, and temporarily fixed; and finally, the broken fracture fragments can be placed. This method is especially suitable for broken ends and when maintaining a stable situation is difficult.[4,24]

The mechanism of heterotopic ossification is not well defined.[22] Heterotopic ossification may be associated with an inaccurate pre-bent reconstruction plate.[11,24] The keys to successful acetabular fracture surgery are precise matching of the femoral head and acetabulum, high integrity of the articular surface, and strong and effective internal fixation.[3,7,12] Hence, it is of great importance to fully understand the fracture morphology and classification and to choose the superior fixation method. Traditional surgical design tends to rely on radiographic or CT images to determine the fracture morphology.[4,5] Even if 3D images are acquired using 3D reconstruction technology, they are read on a two-dimensional plane.[7–9] Therefore, the comprehensive and stereoscopic fracture morphology cannot be obtained from existing imaging data.[10,18] In recent years, 3D CT reconstruction images of fractures have been printed as solid models that can be viewed at any angle.[7] With the 3D model, we can accurately measure the degree of collapse of the articular surface, determine the number and shape of the fracture fragments, perform segmentation of each fragment model, separately print and assemble the fracture fragments, simulate reduction, and determine the position, length, and number of implants.[4,7,12]

Our study should be interpreted with consideration of the following limitations. First, it is a retrospective study and thus contains the inevitable problems that are inherent to this methodology. Patient- and surgeon-related confounders may have been present in our study; however, both groups were well matched, which allowed us to draw conclusions that were not associated with the patients' baseline data. Furthermore, we adjusted for some variables and did not detect substantial residual confounding in the primary analyses. Second, the observational nature of our study makes it difficult to show a direct causal relationship, and this may affect decision-making in clinical outcomes. Third, although most normal human pelvises are symmetrical, factors such as the environment, drugs, and trauma can lead to asymmetric acetabula. We only subjectively visually examined whether the acetabula on both sides were symmetrical; we did not perform an objective symmetry test. If the acetabula were asymmetrical, the mirror imaging model was still used as the reference for pre-bending of the pelvic reconstruction plate and selection of the screw, which may have caused the pre-bent plate to be inaccurate and the length of the screw to be less than ideal. An excessive screw length may damage important vascular nerves, and an insufficient screw length may result in decreased fixation strength. A symmetry test of the bones in the unfractured areas on both sides requires comparison of a large amount of data. We have not yet identified a convenient method for judging the symmetry of the acetabula.

In conclusion, 3D printing mirror model technology in the treatment of acetabular fractures is associated with superior clinical outcomes compared with traditional 3D printing technology. The number of patients in this study was relatively limited, and it was not a prospective study; therefore, analysis of larger samples is needed for more accurate conclusions. Nevertheless, this study revealed accurate treatment of acetabular fractures through 3D printing

mirror model technology, providing a new direction for the surgical treatment of acetabular fractures.

Declaration of conflicting interest

The authors declare that there is no conflict of interest.

Funding

This work was supported by grants from the Shanghai Municipal Health and Family Planning Commission Fund Project (Grant No. 201640057).

ORCID iDs

Weiguang Yu https://orcid.org/0000-0001-6190-8336
Xinchao Zhang https://orcid.org/0000-0002-7618-6396
Guowei Han https://orcid.org/0000-0003-3442-2415

References

1. Hansen E, Marmor M and Matityahu A. Impact of a three-dimensional "hands-on" anatomic teaching module on acetabular fracture pattern recognition by orthopaedic residents. *J Bone Joint Surg Am* 2012; 94: e1771–e1777.
2. Judet R, Judet J and Letournel E. Fractures of the acetabulum: classification and surgical approaches for open reduction. Preliminary report. *J Bone Joint Surg Am* 1964; 46: 1615–1646.
3. Huang Z, Song W, Zhang Y, et al. Three-dimensional printing model improves morphological understanding in acetabular fracture learning: a multicenter, randomized, controlled study. *PLoS One* 2018; 13: e0191328.
4. Li YT, Hung CC, Chou YC, et al. Surgical treatment for posterior dislocation of hip combined with acetabular fractures using preoperative virtual simulation and three-dimensional printing model-assisted precontoured plate fixation techniques. *Biomed Res Int* 2019; 2019: 3971571.
5. Yu AW, Duncan JM, Daurka JS, et al. A feasibility study into the use of three-dimensional printer modelling in acetabular fracture surgery. *Adv Orthop* 2015; 2015: 617046.
6. Letournel E. Acetabulum fracture: classification and management. *Clin Orthop* 1980; 151: 81–106.
7. Citak M, Gardner MJ, Kendoff D, et al. Virtual 3D planning of acetabular fracture reduction. *J Orthop Res* 2008; 26: 547–552.
8. Zhou X, Zhang Q, Song WH, et al. Clinical significance of three-dimensional skeleton-arterial model in the management of delayed reconstruction of acetabular fractures. *BMC Surg* 2018; 18: 30.
9. Chui KH, Chau CCD, Ip KC, et al. Three-dimensional navigation-guided percutaneous screw fixation for nondisplaced and displaced pelvi-acetabular fractures in a major trauma centre. *Int Orthop* 2018; 42: 1387–1395.
10. Zeng CJ, Xing WR, Wu ZL, et al. A combination of three-dimensional printing and computer-assisted virtual surgical procedure for preoperative planning of acetabular fracture reduction. *Injury* 2016; 47: 2223–2227.
11. Venter A, Cioara F, Straciuc O, et al. Three-dimensional CT reconstruction in the imaging of acetabular and pelvic fractures. *Osteoporos Int* 2017; 28: S548.
12. Schwabe P, Altintas B, Schaser KD, et al. Three-dimensional fluoroscopy-navigated percutaneous screw fixation of acetabular fractures. *J Orthop Trauma* 2014; 28: 700–706.
13. Sanchez-Perez C, Rodriguez-Lozano G, Rojo-Manaute J, et al. 3D surgical printing for preoperative planning of trabecular augments in acetabular fracture sequel. *Injury* 2018; 49: S36–S43.
14. Attias N, Lindsey RW, Starr AJ, et al. The use of a virtual three-dimensional model to evaluate the intraosseous space available for percutaneous screw fixation of acetabular fractures. *J Bone Joint Surg Br* 2005; 87B: 1520–1523.
15. Ruan Z, Luo CF, Zeng BF, et al. Percutaneous screw fixation for the acetabular fracture with quadrilateral plate involved by three-dimensional fluoroscopy

navigation: surgical technique. *Injury* 2012; 43: 517–521.
16. Chen X, Chen XH, Zhang GD, et al. Accurate fixation of plates and screws for the treatment of acetabular fractures using 3D-printed guiding templates: an experimental study. *Injury* 2017; 48: 1147–1154.
17. Sebaaly A, Riouallon G, Zaraa M, et al. Standardized three dimensional computerised tomography scanner reconstructions increase the accuracy of acetabular fracture classification. *Int Orthop* 2018; 42: 1957–1965.
18. Keil H, Beisemann N, Schnetzke M, et al. Intraoperative assessment of reduction and implant placement in acetabular fractures-limitations of 3D-imaging compared to computed tomography. *J Orthop Surg Res* 2018; 13: 78.
19. Yu W, Zhang X, Wu R, et al. The visible and hidden blood loss of Asia proximal femoral nail anti-rotation and dynamic hip screw in the treatment of intertrochanteric fractures of elderly high-risk patients: a retrospective comparative study with a minimum 3 years of follow-up. *BMC Musculoskelet Disord* 2016; 17: 269.
20. Zeng X, Zhan K, Zhang L, et al. Conversion to total hip arthroplasty after failed proximal femoral nail antirotations or dynamic hip screw fixations for stable intertrochanteric femur fractures: a retrospective study with a minimum follow-up of 3 years. *BMC Musculoskelet Disord* 2017; 18: 38.
21. Zeng X, Zhang N, Zeng D, et al. Proximal femoral nail antirotation versus dynamic hip screw fixation for treatment of osteoporotic type 31-A1 intertrochanteric femoral fractures in elderly patients. *J Int Med Res* 2017; 45: 1109–1123.
22. Yu W, Zhang X, Zhu X, et al. Proximal femoral nails anti-rotation versus dynamic hip screws for treatment of stable intertrochanteric femur fractures: an outcome analyses with a minimum 4 years of follow-up. *BMC Musculoskelet Disord* 2016; 17: 222.
23. Hinton TJ, Jallerat Q, Palchesko RN, et al. Three-dimensional printing of complex biological structures by freeform reversible embedding of suspended hydrogels. *Sci Adv* 2015; 1: e1500758.
24. Shulaker MM, Hills G, Park RS, et al. Three-dimensional integration of nanotechnologies for computing and data storage on a single chip. *Nature* 2017; 547: 74–78.